Adaptive thresholding of DFT coefficients based on probability distribution of additive noise

ONDREJ RASO, MIROSLAV BALIK
Department of Telecommunications
The Faculty of Electrical Engineering and Communication
Brno University of Technology
Purkyňova 118, Brno 612 00
CZECH REPUBLIC
ondra.raso@phd.feec.vutbr.cz, balik@feec.vutbr.cz

Abstract: - The proposed method of adaptive thresholding uses probability distribution of additive noise signal, by which the input signal is corrupted. The additive noise with non-uniformly distributed power spectral density can be reduced via normalization process. The method is focused on musical signal corrupted by the noise with relative high input signal-to-noise ratio ranging between 20 and 30 dB. The method uses the thresholding of coefficients of Discrete Fourier transform (DFT). Minimal signal distortion should be introduced by this method. In conclusion the method is tested for noise reduction efficiency and size of degradation of processed signal.

Key-Words: - Thresholding, Acoustic noise, Digital filters, Noise reduction, Discrete Fourier transform.

1 Introduction

There are many methods for the reduction of background noise in noisy signals using an appropriate spectrum modification [1][2][3]. Thresholding is one of the most widely used types of spectrum modification [4][5][6]. The fundamentals of threshoding of musical signals together with the half-soft parabolic thresholding rule were described in [7] and [8]. In this article, the thresholding method for noise reduction in signal with a relative high SNR_{IN} value between 20 dB and 30 dB with additional requirements is described.

Three requirements for the proposed method were introduced. The first requirement was the non-uniformly distributed power spectral density of background noise in noisy signal that should be processed. The most of known methods are based on reduction of background noise with uniformly distributed power spectral density (white noise). The second requirement was the maximum reduction of additive noise in noisy signal. And the third requirement was minimal degradation of the musical signal caused by the proposed method. Improving the qualities of the proposed method in the sense of the second requirement is very often in contradiction with improving the qualities in the sense of the third requirement. Hence a compromise is sought between maximal noise reduction and minimal signal degradation [8].

In this article, a thresholding rule will be proposed on the basis of the probability distribution of noise DFT coefficients. This distribution was taken as the basis in order that the thresholding maximally corresponds with the statistic property of additive noise and that the thresholding causes minimal degradation of input musical signal.

If the additive background noise in noisy signal is the white noise, then the estimation of the power of this noise is sufficient for setting the thresholds and the waveform of thresholding rule [7]. These thresholds as well as the waveform of the thresholding rule are the same for all coefficients of the tresholded signal.

If the additive background noise has not uniformly distributed power spectral density, it is necessary to threshold all coefficients of thresholded signal separately, with the same thresholding rule but with differently set thresholds and with a differently set waveform of the thresholding rule. A better solution is to normalize the thresholding coefficients [10]. Due to this normalization, the probability distribution of tresholded coefficients is changed and the same thresholds and waveform of thresholding rule can be used, the same as in the case of white noise. Due to this normalization, only the coefficients of noisy signal which “contain” additive noise are tresholded and the measure of this thresholding is in dependence on the magnitude of the corresponding coefficients of additive noise.

2 Method description

2.1 Method flowchart

The sequence $y(n)$ represents the noisy signal defined by:

$$y(n) = x(n) + m(n), \tag{1}$$

where $x(n)$ is the input signal and $m(n)$ is the additive noise. Figure 1 shows the flowchart of proposed method. The other blocks and signals will be described in the following sections.

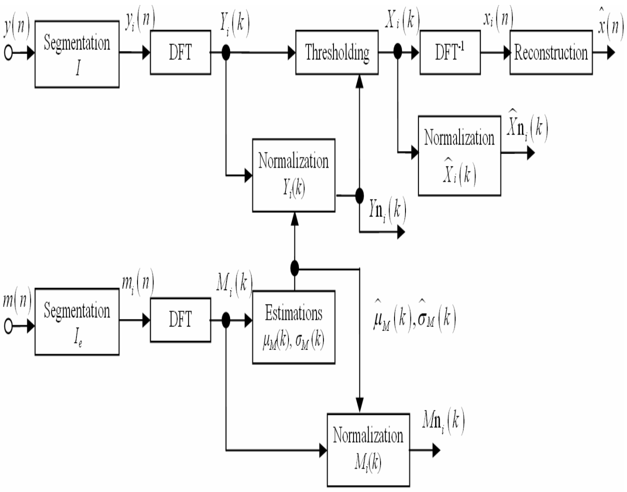

Fig. 1. Flowchart of noise reduction system with polynomial thresholding based on probability distribution of noise signal.

2.2 Segmentation

Segmentation is necessary for processing the long-term sound signal and subsequent application of the thresholding method. Segmentation divides a long-term signal into short segments. The current segment $y_i(n)$ of the signal $y(n)$ is defined as

$$y_i(n) = \left\langle \begin{array}{ll} w(n)\,y(n+iN(1-v)) & \text{for } n = 0,1,...,N-1 \\ 0 & \text{for } n \neq 0,1,...,N-1, \end{array} \right. \quad i = 0,1,...,I-1, \tag{2}$$

where N is the length of segment $y_i(n)$, i is the index of the segment, I is the total number of segments, $w(n)$ is the weighting window, and v is the overlap amount ($v \in (0,1)$), for $v = 0.5$ the overlap is equal to 50 %. The FFT algorithm is used solely for calculating the DFT. Thus it is appropriate to choose the length of the segment as a power of 2. The overlap amount has to comply with the condition $vN \in \mathbb{N}^+$. In the text below, all the variables that belong to the current segment will be indexed with i. The spectrum of the current segment of signal $y_i(n)$ will be marked $Y_i(k)$.

The reconstruction of signal $y(n)$ from its segments $y_i(n)$ is defined as

$$y(n) = \frac{1}{K}\sum_{i=0}^{I-1} y_i\left(n - iN(1-v)\right) \text{ for } n = 0,1,...,N_y - 1, \quad i = 0,1,...,I-1, \tag{3}$$

where N_y is the total length of signal $y(n)$, N is the length of segment $y_i(n)$; and K is a variable dependent on the type of window and on the overlap amount used. The following equation must hold for the weighting windows:

$$\sum_{j=-\infty}^{\infty} w(n - jN(1-v)) = K \qquad for\ \forall n \in \mathbb{Z} \tag{4}$$

For example, the Hanning window (26) with overlap $v = 0.75$ has $K = 2$.

2.3 Discrete Fourier transform

The number of DFT coefficients is equal to the length of processed segment N. This statement results from equations (5) and (6) for forward and backward DFT [11].

$$Y_i(k) = \mathrm{DFT}\{y_i(n)\} = \sum_{n=0}^{N-1} y_i(n)\, e^{-j\frac{2\pi}{N}kn} \tag{5}$$

$$y_i(n) = \mathrm{DFT}^{-1}\{Y_i(k)\} = \frac{1}{N}\sum_{k=0}^{N-1} Y_i(k)\, e^{j\frac{2\pi}{N}kn} \tag{6}$$

2.4 Normalization

After transformation (5) and segmentation (2), equation (1) could be rewritten as

$$Y_i(k) = X_i(k) + M_i(k). \tag{7}$$

The coefficients $M_i(k)$ could be interpreted as stochastic signal $M_i(k) \sim No\,(\mu_{Mi}(k),\sigma_{Mi}(k)^2)$, where No denotes normal probability distribution with mean value $\mu_{Mi}(k)$ and variance $\sigma_{Mi}(k)^2$. In the following text, the premise will be introduced that the additive noise is a stationary. Then it holds $M_i(k) \sim No(\mu_M(k),\ \sigma_M(k)^2)$. After the normalization of coefficients $M_i(k)$ by

$$Mn_i(k) = \frac{M_i(k) - \mu_M(k)}{\sigma_M(k)}, \tag{8}$$

$Mn_i(k)$ will have the probability distribution $Mn_i(k) \sim No(0, 1)$. The mean value and standard deviation will be independent of k.

2.5 Estimations of mean value and standard deviation

The estimation $\hat{\mu}_M(k)$ could be obtained from the equation

$$\hat{\mu}_M(k) = \frac{1}{I_e} \sum_{i=0}^{I_e - 1} M_i(k), \tag{9}$$

where I_e is number of segments from which the estimation $\hat{\mu}_M(k)$ is calculated, and $M_i(k)$ is i-th segment of length N.

Similarly $\hat{\sigma}_M(k)$ could be obtained from the equation

$$\hat{\sigma}_M(k) = \sqrt{\left(\frac{1}{I_e} \sum_{i=0}^{I_e - 1} M_i(k)^2\right) - \hat{\mu}_M(k)^2}. \tag{10}$$

$M_i(k)$ in equations (9) and (10) could be replaced by the coefficients $Y_i(k)$, but in the “quiet parts” only, i.e. in parts where only noise signal remains, i.e. where no input signal is present. It is, for example, a short section before the input signal starts.

After normalization according to (8) with $\hat{\mu}_M(k)$ replaced by $\mu_M(k)$ and $\hat{\sigma}_M(k)$ by $\sigma_M(k)$, equation (8) becomes

$$Mn_i(k) = \frac{M_i(k) - \hat{\mu}_M(k)}{\hat{\sigma}_M(k)}. \tag{11}$$

In a similar way, normalized coefficients $Yn_i(k)$ will be introduced:

$$Yn_i(k) = \frac{Y_i(k) - \hat{\mu}_M(k)}{\hat{\sigma}_M(k)}. \tag{12}$$

After normalization it is possible to use definition for probability density function of stochastic signal (see [7])

$$p\left(\left|Mn_i(k)\right|\right) = \frac{1}{\sqrt{2}} \sqrt{\chi_2\left(\left|Mn_i(k)\right|\right)^2}, \tag{13}$$

where $p(|Mn_i(k)|)$ is the probability density function of the absolute value of additive noise coefficients $Mn_i(k)$, and $\chi_2(|Mn_i(k)|)^2$ is the Chi-square distribution [10] with 2 degrees of freedom shown in figure 2. The probability density function is independent of k and i after normalization.

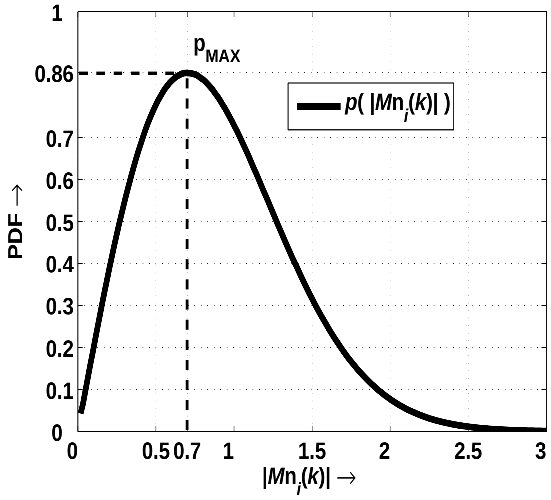

Fig. 2. Probability density function of stochastic signal $|Mn_i(k)|$.

3 Thresholding

Thresholding in this case could be defined as an appropriate form of DFT spectrum modification of noisy signal $y(n)$. The main goal is to find a function δ which performs the estimation of the coefficients $\hat{X}_i(k)$

$$\hat{X}_i(k) = \delta\left(Y_i(k)\right) \approx X_i(k). \tag{14}$$

First, the function $p_{\text{mirorred}}\left(\left|Yn_i(k)\right|\right)$ is defined on the basis of probability distribution $p\left(\left|Yn_i(k)\right|\right)$ of coefficients $Mn_i(k)$

$$p_{\text{mirorred}}\left(\left|Yn_i(k)\right|\right) = \left(\frac{p\left(\left|Yn_i(k)\right|\right)}{p_{\max}} + 1\right). \tag{15}$$

By means of this function, the ideal thresholding rule is introduced:

$$\delta_{\text{ideal}}\left(Y_i(k)\right) = \\ = \begin{cases} 0 & \textit{for} \quad \left|Yn_i(k)\right| \le T_1 \\ Y_i(k)\, p_{\text{mirorred}}\left(\left|Yn_i(k)\right|\right) & \textit{for} \quad T_1 < \left|Yn_i(k)\right| \le T_2 \\ Y_i(k) & \textit{for} \quad \left|Yn_i(k)\right| > T_2 \end{cases}. \tag{16}$$

This function is ideal in the sense that the thresholding between thresholds T_1 and T_2 exactly copies the function $p_{\text{mirorred}}\left(\left|Yn_i(k)\right|\right)$. In figure 3, the ideal thresholding rule $\delta_{\text{ideal}}\left(Y_i(k)\right)$ is shown together with the function $p_{\text{mirorred}}\left(\left|Yn_i(k)\right|\right)$.

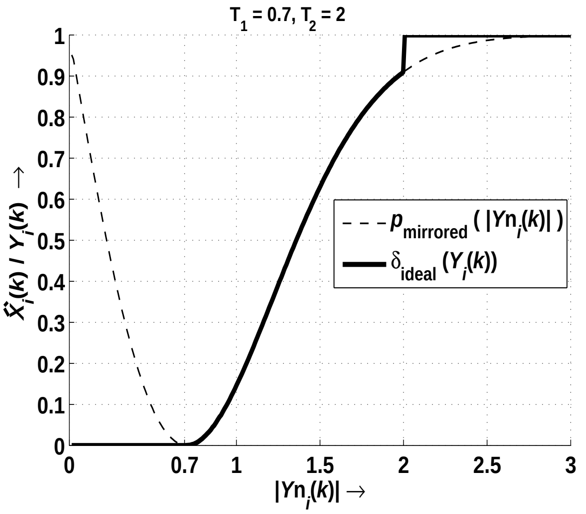

Fig. 3. Ideal thresholding rule.

The function $p_{\text{mirorred}}\left(\left|Yn_i(k)\right|\right)$ was approximated by the 4th-order polynomial

$$p_{poly}\left(\left|Yn_i(k)\right|\right) = 0.2076\left(\left|Yn_i(k)\right|\right)^4 - 1.5995\left(\left|Yn_i(k)\right|\right)^3 + \\ + 4.0711\left(\left|Yn_i(k)\right|\right)^2 - 3.3781\left(\left|Yn_i(k)\right|\right)^1 + 0.8672 \quad (17)$$

This polynomial was proposed for thresholds T_1 = 0.7, T_2 = 3, and with the help of this polynomial the polynomial thresholding rule was defined.

$$\delta_{\text{poly}}\left(Y_i(k)\right) = \\ = \begin{cases} 0 & \text{for} \quad \left|Yn_i(k)\right| \le T_1 \\ Y_i(k)\, p_{\text{poly}}\left(\left|Yn_i(k)\right|\right) & \text{for} \quad T_1 < \left|Yn_i(k)\right| \le T_2 \\ Y_i(k) & \text{for} \quad \left|Yn_i(k)\right| > T_2 \end{cases} . \quad (18)$$

In figure 4, the proposed polynomial thresholding rule $\delta_{\text{poly}}\left(\operatorname{Re}\{Y_i(k)\}\right)$ for the case of $\operatorname{Re}\{Y_i(k)\}$ and for the thresholds T_1 = 0.7 and T_2 = 3 is shown. It should be added, that the coefficients $Y_i(k)$ are complex numbers and not a real numbers.

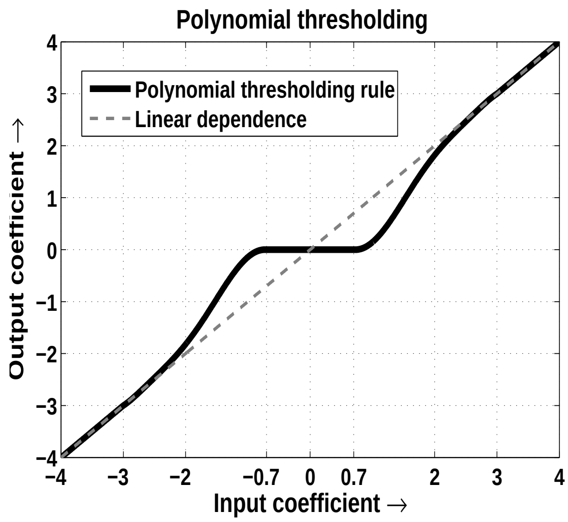

Fig. 4. Polynomial thresholding rule.

In figure 5, the distributions of coefficients Yn_1 and $\widehat{X}n_1(k)$ are shown in the complex plane for the case of thresholding the 1st segment. This segment contains additive white noise only. In this figure, the distribution is shown of: 5a) normalized coefficients $Yn_1(k)$ before thresholding. 5b) normalized coefficients $\widehat{X}n_1(k)$ after thresholding.
The additive noise is a real signal

$$m_i(n) \in \Re \quad \text{for } \forall\ n , \quad (19)$$

so that its transform in the DFT is symmetrical

$$Mn_i(k) = Mn_i^*(N-k) . \quad (20)$$

For this reason and for better notation too, only the first half of sequences of coefficients $Yn_1(k)$ and $\widehat{X}n_1(k)$ is shown only.
Threshold T_1 is shown by the solid-line circle and threshold T_2 is shown by the dashed-line circle. The thresholding of these coefficients is performed according to equation (18). The coefficients with magnitude higher than the threshold T_1 are set to zero. In figure 5a), these coefficients lie inside the solid-line circle. The coefficients with magnitude lower than the threshold T_2 are partially reduced. It is apparent that the coefficients $Yn_1(k)$ are moved to the centre of complex plane in the coordinates [0,0].

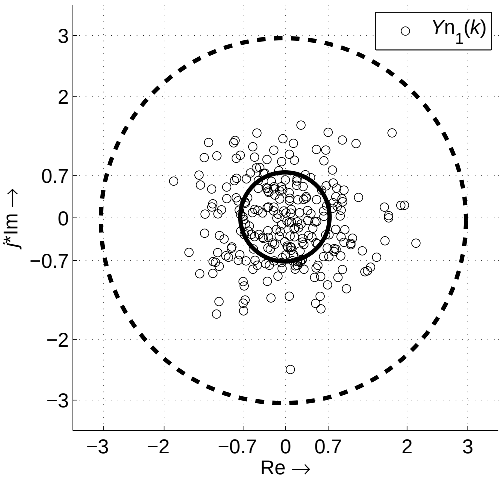

a)

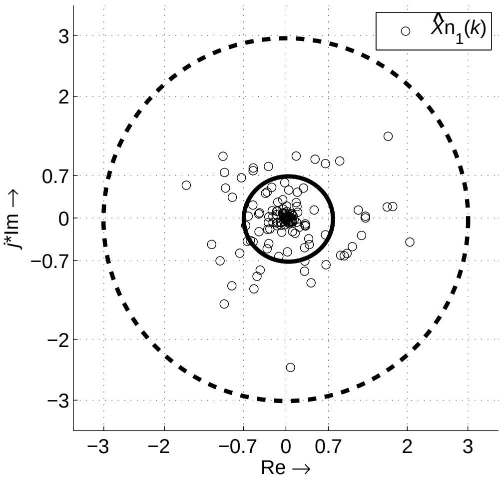

b)

Fig. 5. Example of thresholding a segment which contains additive white noise only: a) normalized coefficients $Yn_1(k)$ before thresholding. b) normalized coefficients $\widehat{X}n_1(k)$ after thresholding.

In figure 6, an example of the spectrogram of additive noise measured in real conditions is shown. It is a record of sound of a fan in a quiet street. This noise will be thresholded. Estimation sequence of mean values $\hat{\mu}_M(k)$ and standard deviations $\hat{\sigma}_M(k)$ are shown in figure 7. From both pictures, it can be read that the frequency components are concentrated into the frequency 13 kHz, and most of the energy is in the range from 0 to 4 kHz.

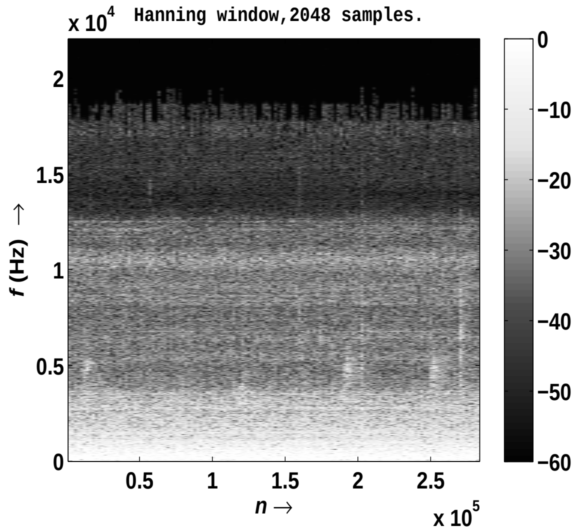

Fig.6. The spectrum of tested additive noise measured in real conditions, sound recording of a fan in the quiet street.

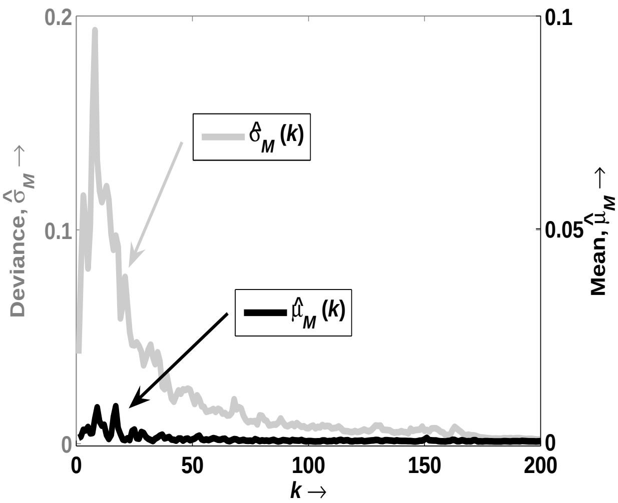

Fig.7. Estimated mean $\hat{\mu}_M(k)$ and standard deviation $\hat{\sigma}_M(k)$ sequences of tested additive noise measured in real conditions, sound recording of a fan in a quiet street.

For this kind of noise, the progress of thresholding and normalization is shown in figures 8a) – d) in the complex plane. In figures 8a) the chosen segment $i = 110$ with length $N = 512$ samples before thresholding $Y_{110}(k)$ is shown. All of these coefficients represent additive noise, therefore these coefficients have to be reduced as much as possible. Figures 8b), these coefficients are shown after normalization $Yn_{110}(k)$. The inner solid-lines circle again represents the threshold T_1 and the outer dashed-line circle represents the threshold T_2. In figures 8c), the normalized coefficients $\widehat{X}n_{110}(k)$ after thresholding are shown, and in figures 8d), the non-normalized coefficients $\widehat{X}_{110}(k)$ after thresholding are shown.

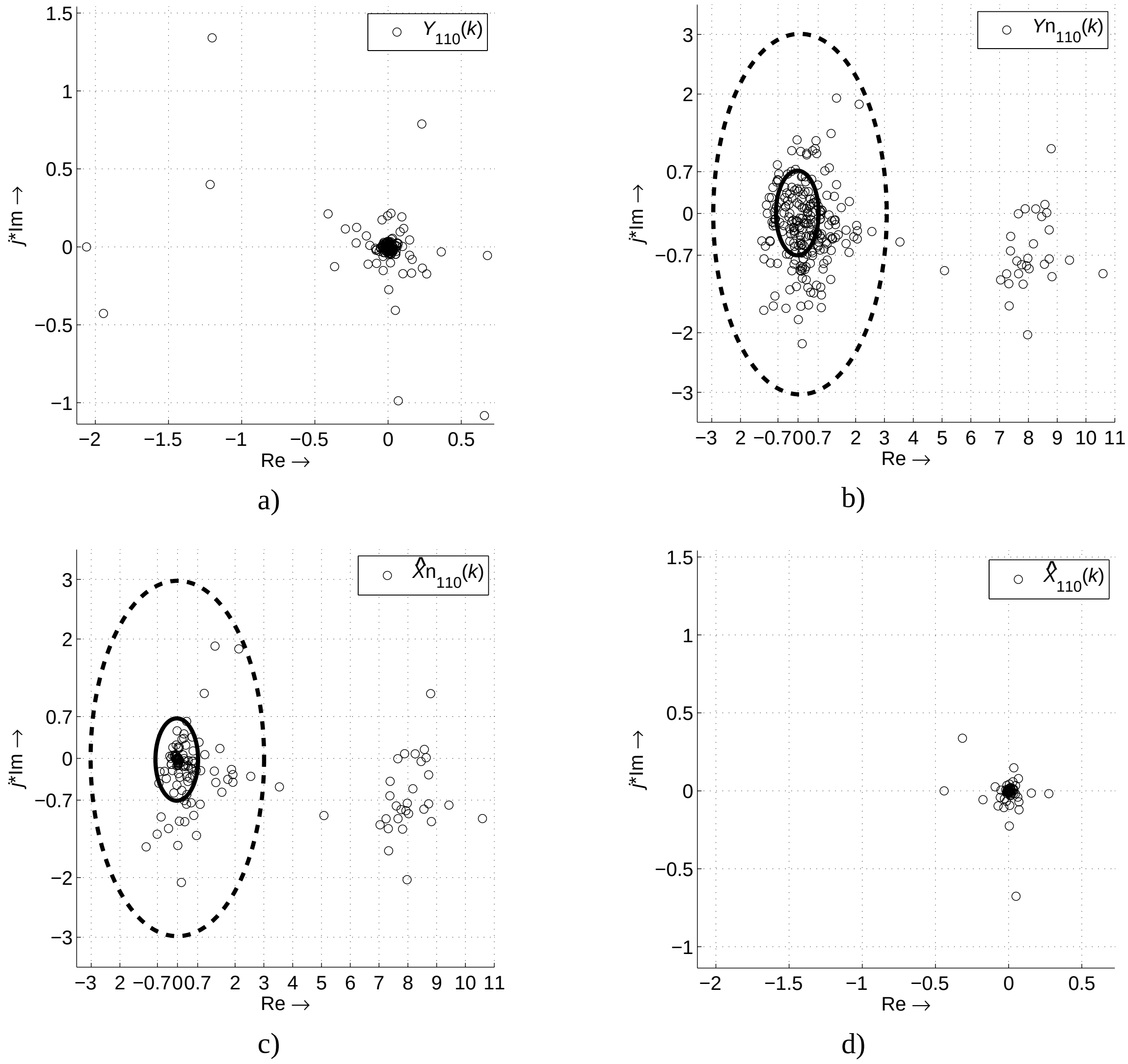

Fig. 8. Example of segment thresholding: a) $Y_{110}(k)$, coefficients before normalization, b) $Yn_{110}(k)$, coefficients after normalization, c) $\widehat{X}n_{110}(k)$, normalized coefficients after thresholding, d) $\widehat{X}_{110}(k)$, non-normalized coefficients after thresholding.

In these figures, the progress of thresholding and normalization of a chosen segment containing only the additive noise is shown. As well as in figures 5a) - b), the coefficients are moved to the centre of Z-plane in the coordinates [0,0]. Due to normalization (8), the same waveform of the thresholding rule with the same thresholds could be used even for the case of additive noise with non-uniformly distributed power spectral density.

4 Test results

The proposed polynomial thresholding rule was tested for additive noise $m(n)$ reduction efficiency and the measure of the degradation of input signal $x(n)$ was monitored at the same time. The estimate of mean value $\widehat{\mu}_M(k)$ and standard deviation $\widehat{\sigma}_M(k)$ sequence of additive noise was calculated (9)(10) from $I_e = 610$ segments, with length $N = 2048$ samples. These segments are not displayed in the following spectrograms. These segments were not included in equations for the calculation of *SNR* and *SNRE* according to (22) (23) and (24) either.

Signal $\hat{x}(n)$ is an estimate of the signal $x(n)$ according to

$$\hat{x}_i(n) = DFT^{-1}\left(\hat{X}_i(k)\right) = DFT^{-1}\left(\delta\left(Y_i(k)\right)\right) \approx x_i(n). \quad (21)$$

The *SNRE* (24) value, which was calculated from SNR_{IN} (22) and SNR_{OUT} (23), was used to define the amount of noise reduction in the signal $y(n)$. The difference between the *SNR* values before and after thresholding was calculated.

$$SNR_{\mathrm{IN}} = 10\log_{10}\frac{\sum_{n=0}^{N_x-1} x^2(n)}{\sum_{n=0}^{N_x-1}\left(y(n)-x(n)\right)^2} \tag{22}$$

$$SNR_{\mathrm{OUT}} = 10\log_{10}\frac{\sum_{n=0}^{N_x-1} x^2(n)}{\sum_{n=0}^{N_x-1}\left(\hat{x}(n)-x(n)\right)^2} \tag{23}$$

$$SNRE = SNR_{\mathrm{OUT}} - SNR_{\mathrm{IN}} \tag{24}$$

The tests were performed on a musical signal containing viola play. The additive noise $m(n)$ is the recording of a fan sound in a quiet street. The musical signal represents the signal $x(n)$ and additive noise $m(n)$ in (1). The frequency sampling of this signal is $f_s = 44.1$ kHz, the length of the whole signal is $N_y = 241\,664$ samples. Both polynomial thresholding (18) and hard thresholding (25) were tested. The hard thresholding is shown in figure 9.

$$\delta_{\mathrm{h}}\left(Y_i(k)\right) = \\ = \begin{cases} 0 & for \quad \left|\mathrm{Yn}_i(k)\right| \le T_{\mathrm{h}} \\ Y_i(k) & for \quad \left|\mathrm{Yn}_i(k)\right| > T_{\mathrm{h}} \end{cases}. \tag{25}$$

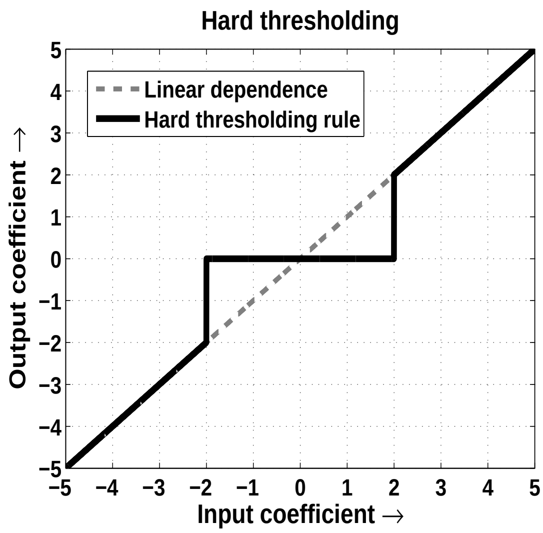

Fig. 9. Hard thresholding rule.

The threshold T_{h} of the hard thresholding rule was defined as $T_{\mathrm{h}} = \frac{T_1 - T_2}{2}$. The Hanning window (26) was used for the segmentation (2).

$$w(n) = \begin{cases} 0.5\left(1-\cos\left(2\pi\frac{n}{N}\right)\right) & \text{for } n = 0,1,\ldots,N-1 \\ 0 & \text{for } n \ne 0,1,\ldots,N-1 \end{cases}. \tag{26}$$

The other settings used are specified in Table 1. In the Table in the case of thresholding rule called “*Polynomial 2*“, the music noise filter $SW(i)$ with length equal to 2 samples [8] was used in addition to the higher value of segment length N and higher overlap v.

TABLE I
NOISE REDUCTION TEST RESULTS

Threshold rule	*Settings*	*Thresholds*	SNR_{OUT} [dB]	*SNRE* [dB]
Hard	$N = 2048$, $v = 0.5$	$T_{\mathrm{h}} = 1.85$	**22.3**	**2.3**
Polynomial 1	$N = 2048$, $v = 0.5$	$T_1 = 0.7$, $T_2 = 3$	**23,6**	**3.6**
Polynomial 2	$N = 4096$, $v = 0.75$	$T_1 = 0.7$, $T_2 = 3$	**25,3**	**5.3**

All of these changes increased the computational complexity but they also increased the value of *SNRE* from 3.6 dB to the best value 5.3 dB from Table 1.

In following figures 10 and 11 the spectrograms of test signals $x(n)$, $y(n)$ and $\hat{x}(n)$ are shown.

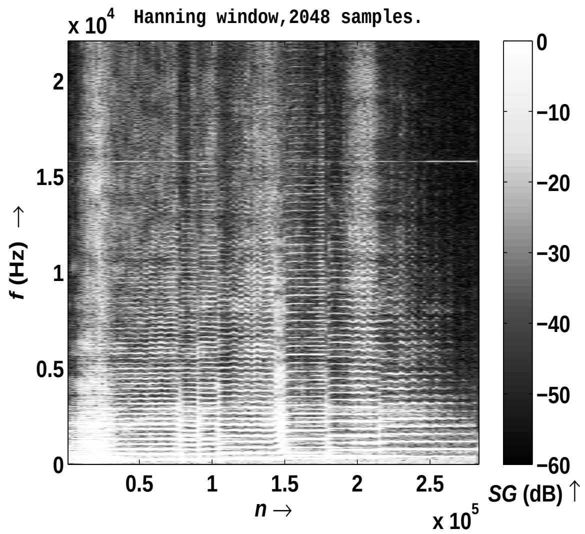

Fig. 10. Spectrogram of tested input signal $x(n)$.

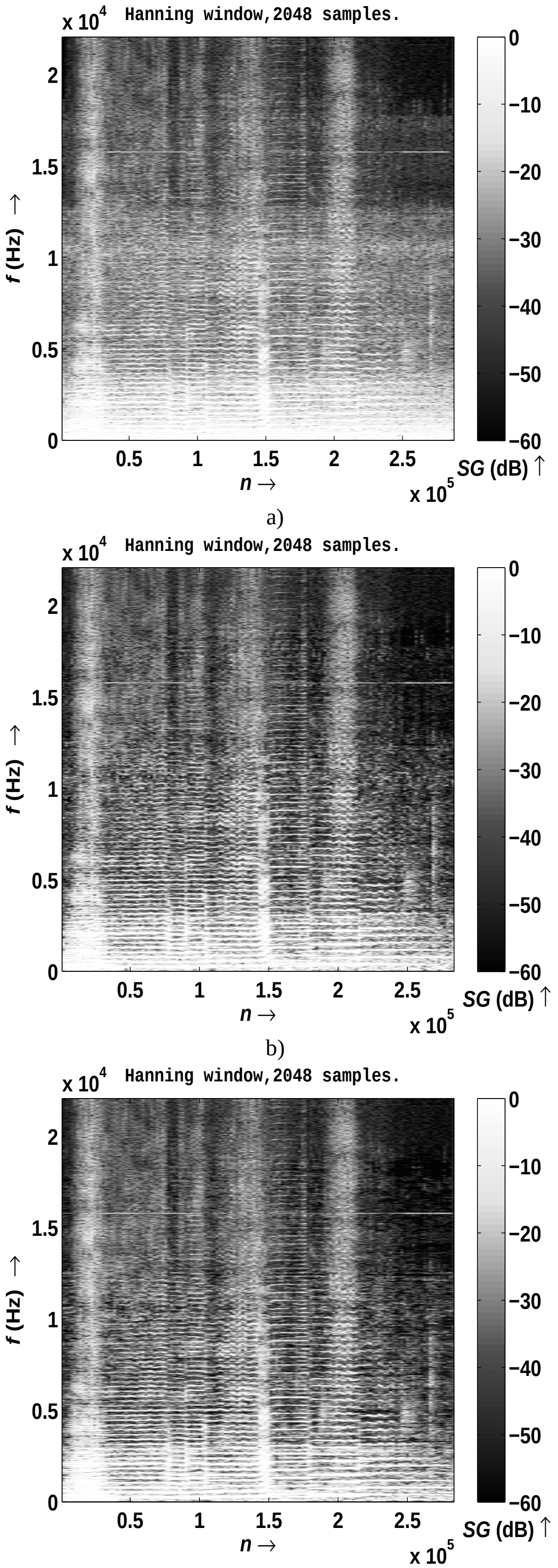

Fig. 11. Spectrograms of tested signal: a) noisy signal $y(n)$ to be processed, b) the signal $\hat{x}(n)$ after "polynomial 1" thresholding, c) the signal $\hat{x}(n)$ after "polynomial 2" thresholding.

In the design of polynomial thresholding, the requirement was to have the smallest possible input signal degradation by the thresholding method. A higher value of *SNRE* does not always mean a better listening quality. The higher harmonic components of musical instruments can be suppressed by thresholding or these higher harmonic components in the spectrum can even be totally removed. For listeners this spectrum modification is a much more disturbing effect than background noise.

To test the degradation caused by the thresholding rule, the input signal $x(n)$ without the presence of noise signal is thresholded in order to show the degradation measure in the spectrograms. The spectrograms of the signal $\hat{x}(n)$ after thresholding are shown in figures 12 and 13. The thresholds were set to the same value as in the case of white noise with SNR_{IN} = 25 dB [7].

In comparison with figure 10, the input signal $x(n)$ was in both case degraded as a result of thresholding a clear signal by the thresholding rule.

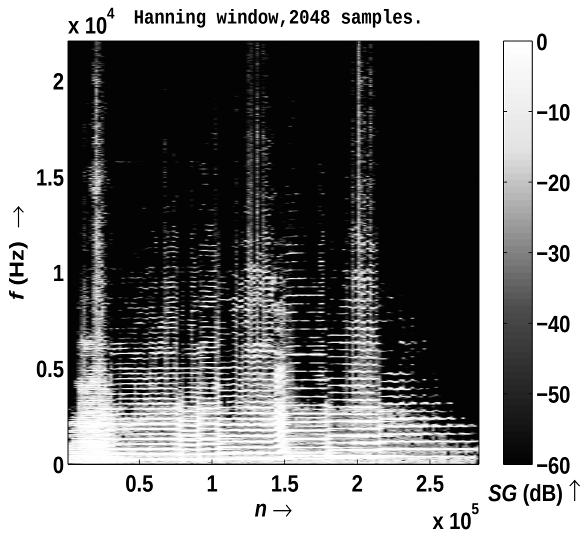

Fig. 12. Comparison of signal degradation caused by the thresholding rule (settings for the white noise) after the polynomial thresholding

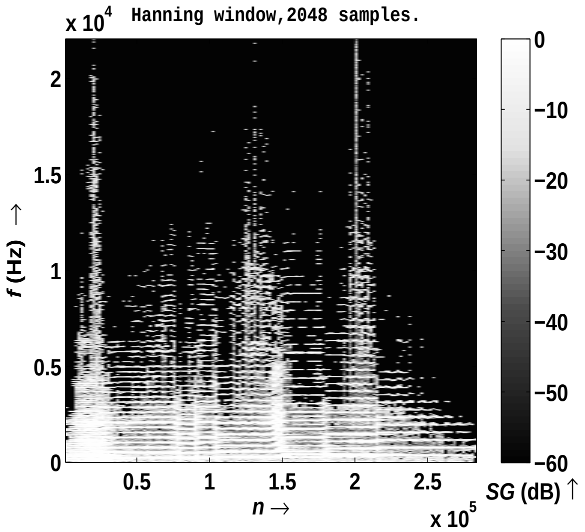

Fig. 13. Comparison of signal degradation caused by the thresholding rule (settings for the white noise) after hard thresholding

From a comparison of the two spectrograms (figures 12 and 13)), it can be seen that the spectrum after polynomial thresholding is more detailed. In polynomial thresholding, there are no such sharp changes and the higher part of the spectrum is much more detailed.

In figure 14, the spectrogram of input signal $x(n)$ after processing by "polynomial 1" thresholding is shown.

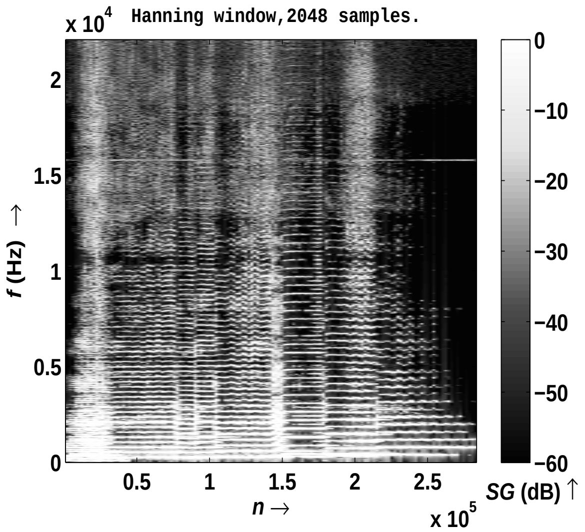

Fig. 14. Degradation of the input signal caused by the polynomial thresholding rule (setting for the noise from a fan in a quiet street).

The sound of a fan in the quiet street is used as noise signal to set the thresholds in this case. The thresholds were set for $SNR_{IN} = 20$ dB. Due to normalization (12), only the coefficients $Y_i(k)$ that contain noisy component are tresholded. Comparing figures 10 and 14, it is possible to see that frequency components from 13 kHz upwards are left almost without change.

5 Acknowledgements

Research described in the article was supported by the Czech Ministry of Education in research program NPVII under grant No. 2E08035 and by the research program MSM 0021630513.

6 Conclusion

In the article the method for additive background noise reduction in noisy musical signal was described. The method chosen is the polynomial thresholding of DFT coefficients. The method is always used for the current segment of the signal being processed. The process of segmentation, the weighting of segments and the process of backward reconstruction were described. Further the probability distribution of additive noise was mathematically described and the polynomial thresholding rule was proposed on the basis of this probability distribution. Because normalization process was used, the proposed polynomial thresholding rule could be applied to the additive noise with non-uniformly distributed power spectral density.

The rest of the article deals with the testing the proposed polynomial thresholding rule on musical signals to which the real noise type was added. This real noise type was the sound of a fan on a quiet street and it had non-uniformly distributed power spectral density.

During a testing, the noise reduction efficiency was tested and then the measure of signal degradation caused by the thresholding rule was monitored at the same time. The *SNRE* value, which was calculated from SNR_{IN} and SNR_{OUT}, was used to define the size of noise reduction in the signal $y(n)$. Hard thresholding together with polynomial thresholding was tested too. After the tests are done, it is possible to see that polynomial thresholding marked as "Polynomial 2"reached the highest *SNRE* value.

In the second part of testing, the degradation caused by the threshold rule was tested. The input signal $x(n)$ without the presence of noise signal was tresholded in order to show the measure of degradation in the spectrograms. Because the polynomial thresholding rule was proposed on the basis of probability distribution of additive noise, the spectrogram after thresholding by this thresholding rule is more detailed in comparison to hard thresholding.

References:

[1] VASEGHI, S. V,. *Advanced Digital Signal Processing and Noise Reduction*. 2nd edition. New York : Wiley, 2000. 473 p. ISBN 0-471-62692-9.

[2] CHAVAN M. S., AGARWALA RA., UPLANE M.D., Design and implementation of Digital FIR Equiripple Notch Filter on ECG Signal for removal of Power line Interference. *WSEAS TRANSACTIONS on SIGNAL PROCESSING 2008*. Vol.4, ISSN: 1790-5052, pp 221-230.

[3] ARIGELA S., ASARI V. K., A Locally Tuned Nonlinear Technique for Color Image Enhancement. *WSEAS TRANSACTIONS on SIGNAL PROCESSING 2008*. Vol.4, ISSN: 1790-5052, pp 514-519.

[4] JANSEN, M., *Noise reduction by wavelet thresholding*. New York : Springer, 2001. 191 p. ISBN 0-387-95244-6.

[5] KOZUMPLÍK, J., *Vlnkové transformace a jejich využití pro filtraci signálů EKG* (in Czech). Inaugural dissertation, Brno University of technology, 2004. 81 p.

[6] RAJMIC, P., *Exploitation of the wavelet transform and mathematics statistic for separation signals and noise* (in Czech: *Využití waveletové transformace a matematické statistiky pro separaci signálu a šumu*). PhD Thesis, Supervizor: Prof. Ing. Zdeněk Smékal, CSc., Brno University of technology, 2004. 106 p.

[7] RÁŠO O., BALÍK M., Half-soft parabolic thresholding of DFT coefficients. *Proc. 32nd International Conference Telecommunication and Signal Processing 2009*, Dunakiliti, Hungary, 2009, pp. 1-6. ISBN:978-963-06-7716-5.

[8] BALÍK M., RÁŠO O., Sound artifacts caused by the thesholding method. *The IASTED International Conference on Modelling, Simulation, and Identification (MSI 2009)*, Beijing, China, 2009, pp. 1-8. ISBN: 978-0-88986-810-6.

[9] SCHIMMEL J., MISUREC J., Analytic Solution of Spectrum Changes in Simple Nonlinear Systems without Memory, Used in Digital Audio Signal Processing. *Proc. 7th WSEAS International Conference on CIRCUITS, SYSTEMS, ELECTRONICS, CONTROL and SIGNAL PROCESSING (CSECS'08)*, Puerto De La Cruz, Spain, 2008, pp. 191-196. ISBN:978-960-474-035-2.

[10] BAŠTINEC, J., ZAPLETAL J., *Statistic, operations research, stochastic processes* (in Czech: *Statistika, operační výzkum, stochastické procesy*). Lecture notes, Brno University of technology, 2007. 161 p.

[11] SMÉKAL, Z., *Digital signal processing* (in Czech: *Číslicové zpracování signálu*). Lecture notes, Brno University of technology, 2009. 201 p.

[12] MALLAT, S., A *Wavelet Tour of Signal Processing*. 2nd edition. New York: Academic Press, 1998. 637 p. ISBN 0-12-466606-x.

[13] HÄNSLER, E. S., Gerhard. *Topics in Acoustic Echo and Noise Control: Selected Methods for the Cancellation of Acoustic Echoes, the Reduction of Background Noise, and Speech Processing*. Berlin-Heidelberg-New York: Springer, 2006. 642 p. ISBN 10 3-540-33212-x.

[14] LINHARD K., HAULICK T., Spectral noise subtraction with recursive gain curves. *Proc. ICSLP '98*, 1998, pp. 1479-1482.

[15] SHAH V.,Inharmonic Dispersion Tunable Comb Filter Design Using Modified Iir Band Pass Transfer Function. *WSEAS TRANSACTIONS on SIGNAL PROCESSING 2008*. Vol.4, ISSN: 1790-5052, pp 381-387.